reaction. It is unfortunate that decays to this level were not seen in the $Si^{29}(p,\gamma)P^{30}$ reaction.[3] It is possible, however, that they were overlooked in the necessarily complex fitting of de-excitation gammas into the level structure known from the (d,α) reaction.

Such an inversion as proposed would really not be unusual in P^{30}. Similar inversion is known in Cl^{34},[10] and suspected in K^{38} [11,12] and Sc^{42}.[13] Actually the cross-over is expected soon after mass 26.[14] Final confirmation of this suggested interpretation must await a careful re-examination of $Si^{29}(d,n)P^{30}$ and $P^{30}(\beta^+)Si^{30}$ now being undertaken.

The Si^{30}-P^{30} mass difference calculated on the basis of the ground-state Q value of the $Al^{27}(\alpha,p)Si^{30}$ and $Al^{27}(\alpha,n)P^{30}$ reactions is 4.30±0.06 Mev. This compares quite favorably with the reported $P^{30}(\beta^+)Si^{30}$ Q value of 4.26 Mev.[9]

TABLE I. Q values obtained in this analysis.

Group	Reaction	Q (Mev)	Excitation (Mev)	Probable T
a	$Al^{27}(\alpha,n)P^{30}$	−2.70±0.06	0	1
b		−2.96±0.06	0.26	0
d		−3.59±0.06	0.89	1, 0
f		−4.43±0.04	1.73	0
g		−4.96±0.04	2.26	0
c	$Al^{27}(d,n)Si^{28}$	0	...	...

ACKNOWLEDGMENTS

The authors wish to thank Professor G. Breit for several helpful discussions. Thanks are also due to Miss Marsha Davis for her assistance in the analysis of the data.

[10] W. Arber and P. Stähelin, Helv. Phys. Acta **26**, 433 (1953).
[11] D. Green and J. R. Richardson, Phys. Rev. **101**, 776 (1956).
[12] P. Stähelin, Helv. Phys. Acta **26**, 691 (1953).
[13] J. A. R. Cloutier and R. Henrikson, Can. J. Phys. **35**, 1190 (1957).
[14] S. A. Moszkowski and D. C. Peaslee, Phys. Rev. **93**, 455 (1954).

PHYSICAL REVIEW VOLUME 117, NUMBER 2 JANUARY 15, 1960

Photoproduction of Neutral Pions at Energies 600 to 800 Mev*

R. M. WORLOCK†
California Institute of Technology, Pasadena, California
(Received August 11, 1959)

The photoproduction of neutral π mesons from hydrogen has been studied at the California Institute of Technology Synchrotron Laboratory by detecting recoil protons from a liquid hydrogen target irradiated by the synchrotron bremsstrahlung beam. The recoil protons were detected by a five-counter telescope. Data were taken at proton laboratory angles of 19°, 30°, 40°, 50°, and 60° at proton energies corresponding to photon energies of 600, 700, and 800 Mev. Angular distribution data are produced at these three energies and fitted with functions of the form: $A+B\cos\theta_\pi'+C\cos^2\theta_\pi'$. These functions are qualitatively like those at lower energies; B is small and $-A/C$ is roughly 1.25. The total cross section is found to have a minimum at about 600 Mev, being slightly larger at 700 and 800 Mev.

I. INTRODUCTION

THE photoproduction of π mesons from hydrogen has been the subject of extensive study at this laboratory and elsewhere.[1] The predominance of a single state of total angular momentum $\frac{3}{2}$ and isotopic spin $\frac{3}{2}$ in the pion-nucleon interaction and use of the scattering phase shifts from pion-nucleon scattering data in a phenomenological model have made possible a satisfactory understanding of meson production by photons up to about 400 Mev.[2] A meson theory calculation by Chew and Low[3] has also been successful in explaining the general features of the process in this energy region.

The experiment described here was carried out to extend the existing data on π^0 photoproduction in hydrogen to higher energies. Little theory currently exists which attempts to explain pion phenomena above about 400 Mev. Still, it is worthwhile to have higher energy data for phenomenological comparisons with charged meson photoproduction and pion-nucleon scattering. Briefly stated, the results of this experiment are that up to 800 Mev the angular distributions are qualitatively the same as at lower energies. The total cross section does not continue to fall rapidly with increasing energy but goes through a minimum at about 600 Mev, and then rises slightly at 700 and 800 Mev.

II. EXPERIMENTAL TECHNIQUE

The method used in this experiment was to count the recoil protons from the reaction $\gamma+p\rightarrow p+\pi^0$ by means of a counter telescope. This method has a good counting rate and is simple, but suffers from the fact

* This work was supported in part by the U. S. Atomic Energy Commission.
† Now at Electro-Optical Systems, Inc., Pasadena, California.
[1] For a review of previous work, see L. J. Koester and F. E. Mills, Phys. Rev. **105**, 1900 (1957).
[2] Watson, Keck, Tollestrup, and Walker, Phys. Rev. **101**, 1159 (1956).
[3] G. F. Chew and F. E. Low, Phys. Rev. **101**, 1579 (1956).

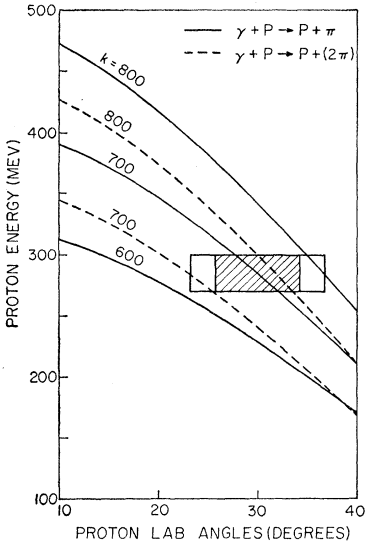

FIG. 1. Proton kinematics for single and double pion photoproduction. The pair production curve is calculated for the case where the two pions go off together. The rectangle represents a typical telescope "window." The outer rectangle indicates the full width of the angular resolution, while the inner rectangle indicates the angular resolution width at half-height. About 85% of the counting rate comes from the inner rectangle.

that protons may come from reactions other than the desired one. From hydrogen, the offending reactions are:

$$\gamma+p \rightarrow p+\gamma'$$
$$\rightarrow p+\pi^+ +\pi^-$$
$$\rightarrow p+\pi^0+\pi^0$$
$$\rightarrow p+3 \text{ or more mesons.}$$

The Compton process has a small enough cross section to be an unimportant source of error; the multiple pion process cross sections are much larger, but by taking suitable precautions and making corrections based on available data, the error introduced is not excessive. These reactions will be considered more quantitatively later.

Figure 1 shows some pertinent kinematics of the photoproduction reaction. Since a counter telescope counts protons in specified angular and energy ranges, a given telescope setting defines a rectangle on this diagram. The probability of being counted is not necessarily the same for protons from all points inside the rectangle if the rectangle size includes the effects of a target of finite size. The solid lines represent the single production process, $\gamma+p \rightarrow p+\pi^0$, and the dotted lines represent pair production, $\gamma+p \rightarrow p+(2\pi)$, where the parentheses mean that the two pions go off together. This case is drawn since it is the case requiring the minimum gamma-ray energy for a given proton energy and angle. Thus, for synchrotron energy E_0, protons from the single process are energetically possible at all points below the $k=E_0$ line for single production and protons from the pair process are energetically possible at all points below the $k=E_0$ line for pair production. To operate without a contamination by the pair process, then, the rectangle defined by the telescope must fit between the single production curve and the pair production curve for the particular machine energy chosen. It must lie above the pair curve so that no protons from the pair process can be present, and below the single production curve so that the desired protons will be present.

As can be seen from the figure, it would be very difficult to operate in this manner. Decreasing the angular and energy resolution sufficiently would make the counting rate prohibitively low. For this reason, it was decided to operate in a more conventional manner using angular resolutions of 8 to 14 degrees (full width) and proton energy resolutions of 10 to 30 Mev. Assuming a thin-target bremsstrahlung spectrum, E_0 would optimally have been set so that the $k=E_0$ line for single production intersected the upper right-hand corner of the telescope rectangle, thus minimizing the pair contamination without interfering with the single production. However, at the time of the experiment the spectrum was not known to have a sharp cutoff. In addition, E_0 had to be determined by compromise so that several experiments could run simultaneously. It turned out to be about 120 Mev above the average energy being measured, which was usually enough to cover the resolution of the telescope while keeping the pair contamination down to a reasonable value. The magnitude of this contamination and correction for it will be discussed in more detail later.

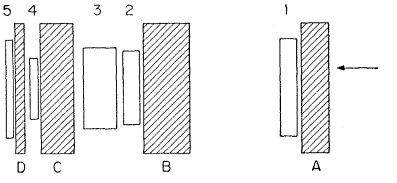

FIG. 2. Plan view of counter telescope (schematic). A, B, C, and D are absorbers. 1, 2, 3, 4, and 5 are counters. Protons travel in the direction of the arrow.

The telescope consisted of five counters and associated absorbers as shown in Fig. 2. Counters 2, 4, and 5 make up a standard three scintillation counter telescope which operates as follows: the range of a counted particle is determined within a certain ΔR by placing counters 2 and 4 in coincidence and counter 5 in anticoincidence. Protons producing the proper coincidence event are identified by their specific ionization in counter 2. Counter 3, the Čerenkov counter, is sensitive to electrons and is placed in anticoincidence to discriminate against multiple electron events which are capable of producing proton-like pulses in a counter telescope. Counter 1 is placed in coincidence with a minimum of absorber in front of it. By demanding a proton-like pulse it serves two purposes: (1) It discriminates against mesons making the proper coincidence event, which, due to the Landau distribution in energy loss in counter 2, appear to be protons, and (2) it discriminates against secondary protons made in absorber B by uncharged or lightly ionizing particles. Calculation shows that the pion and recoil neutron flux produces enough stars in absorber B with proton prongs to cause appreci-

able error if no precautions are taken. The experimental area arrangement, liquid hydrogen target, and beam monitoring equipment have been discussed elsewhere[4] and need not be discussed further here.

Defining U=Mev/BIP [5] and E_0=bremsstrahlung upper limit, the number of photons/BIP at energy k in an interval dk is $N(k)dk=(U/E_0)B(k,E_0)dk/k$. $B(k,E_0)$ contains the deviations in the spectrum from a $1/k$ dependence and is normalized so that $\int_0^{E_0} B(k,E_0)dk=1$. On the basis of pair spectrometer measurements by Donoho, Emery, and Walker,[6] $B(k,E_0)$ is assumed constant with a value 0.90 for values of k/E_0 between 0.6 and 1.0. This is a simple approximation to the theoretical thin-target spectrum and gives results indistinguishable from the latter for an experiment with an energy resolution as poor as the present one. The pair spectrometer measurements were of limited accuracy

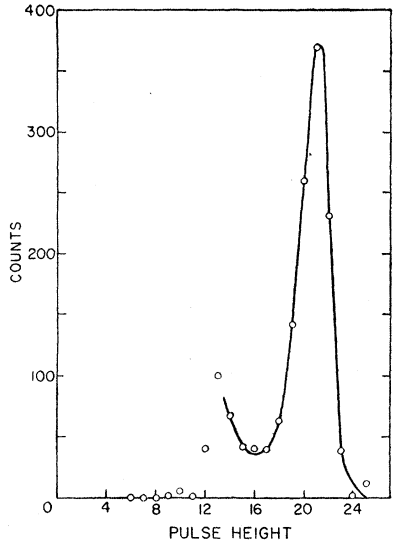

FIG. 3. Proton pulse-height spectrum in counter 2. Proton energy is 332 Mev and proton laboratory angle is 30°.

because of a troublesome background, but showed that the spectrum was much closer to that expected for a thin target than to that expected from a target of the nominal thickness (0.2 radiation length) of the one in the synchrotron.[7]

The beam intensity distribution over the target was measured by Vette by exposing in the beam electron-sensitive nuclear emulsion plates whose positions relative to the target cylinder were known. After development, measurements were made with a densitometer and a beam intensity distribution function determined for several different machine energies. The role of this function in the calculation of cross sections is discussed later.

Since the photoproduction reaction is a two-body process, the laboratory photon energy and center-of-mass meson angle may be calculated when the proton laboratory energy and angle are known. The proton energy determines the range.[8] Absorbers A, B, C, and D (Fig. 2) were chosen as follows: Absorber D was arrived at by a compromise between high counting rate (counting rate varies linearly with D) and good energy resolution. Absorber C was chosen to give close to optimum separation of meson and proton peaks as seen in counter 2. Absorber A was a low-Z material such as CH_2 or aluminum to minimize scattering and secondary proton production; only enough was used to keep the counting rate in counter 1 down to a reasonable figure. Last of all, absorber B was chosen to bring the total mean range up to the desired value. Copper blocks, 4 in. square, were used for absorbers B, C, and D.

A typical pulse-height spectrum from counter 2 as recorded by the pulse-height analyzer is shown in Fig. 3. The absence of the meson peak is due to the high bias setting on counters 1 and 2. About a third of the width can be ascribed to the proton energy spread acceptable by the telescope; the rest is due to the resolution of the counter. At larger proton angles, the peak to valley ratio was slightly better and at smaller angles it was somewhat worse.

Data were taken with and without hydrogen in the target at proton energies corresponding to photon energies of 600, 700, and 800 Mev and proton laboratory angles of 19°, 30°, 40°, 50°, and 60°. Run lengths were divided between full target and empty target to give minimum statistical errors for a given total number of BIP's. At 19°, 30°, and 40° enough data were taken to give approximately 5% statistics; at 50° and 60°, 7% statistics were obtained. The machine energy E_0 and the ion chamber pressure and temperature were monitored so that all runs could be corrected to STP and corrected for variations in E_0 from run to run.

The ratio of empty target counting rate to full target counting rate varied between 15% and 50%, with the higher values occurring at the forward proton angles. At proton angles of 50° and 60°, it was possible to erect lead walls which prevented protons produced in the Mylar vacuum window from being counted.

To maintain the contributing photon energy interval at a reasonable value, the energy and angular resolution of the telescope had to be changed as a function of proton angle and energy. The angular resolution, produced both by the width of the defining counter in the telescope and by the finite size of the target, was changed by varying the distance from the target to the defining counter and by using defining counters of different widths. The proton energy resolution was changed by varying ΔR as described earlier.

[4] J. I. Vette, Phys. Rev. **111**, 622 (1958).
[5] BIP stands for "beam integrator pulse" and is used as the unit of integrated beam energy.
[6] Donoho, Emery, and Walker (private communication).
[7] More recent measurements, still incomplete, confirm the earlier thin-target results.
[8] Rich and Madey, University of California Radiation Laboratory Report UCRL-2301, 1954 (unpublished).

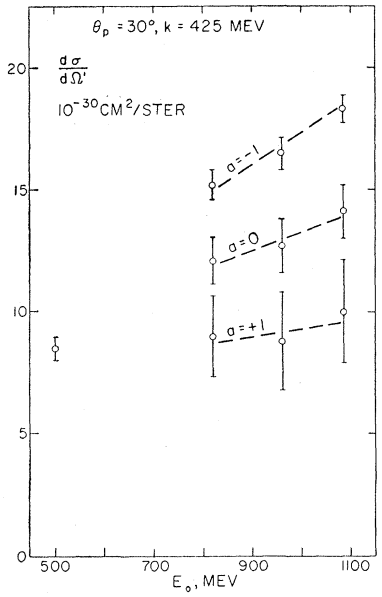

FIG. 4. Typical result of measurement made to determine the effect of pion pair production on proton counting rates. Different sets of points correspond to different values of the parameter a. Since the correction is proportional to $(1+a)$, $a=-1$ is used to label the uncorrected data.

III. DATA REDUCTION

The result of the telescope operation is a set of proton counting rates: counts/BIP as a function of proton energy and angle. The first step in the data reduction is to apply to these raw data corrections for various effects which cause differences from the "true" counting rate. These corrections, which will be discussed below, are: (1) absorption, (2) pion pair process contamination, (3) Compton process, (4) scattering, and (5) accidental coincidence and dead time.

The correction for absorption of protons in the absorbers and counters was calculated (assuming the entire proton path to be in copper) from the results of Fernbach, Serber, and Taylor[9] who considered the problem of scattering of a neutron wave by a sphere of material characterized by an absorption coefficient and an index of refraction. Using the np and pp scattering cross sections quoted by Rossi[10] and including a correction for the presence of the target nucleon in a nucleus as calculated by Goldberger,[11] the absorption cross section for protons in copper was calculated as a function of energy. These cross sections are consistent with the measured values quoted by Millburn *et al.*[12] The calculated cross section was integrated to obtain the fraction of protons of a given range that come to rest in copper without being absorbed.

Our knowledge of the pion pair process at the present is rather fragmentary, due both to lack of any high-energy pion theory and the difficulty of obtaining experimental data on three-body reactions. However, the results of Bloch[13] for the process $\gamma+p\rightarrow p+\pi^+ +\pi^-$ provide a basis for calculating a correction to the data of this experiment. Bloch obtained π^- energy spectra at two angles for four values of E_0, the bremsstrahlung limit. By subtraction, these data yield the cross section $d^2\sigma/dT_{\pi^-}d\Omega'$ at three energies for each of the two angles. Integrating over the π^- energy gives $d\sigma/d\Omega'$ which, within the statistics, is isotropic in the c.m. system and is a constant function of k between 660 and 1000 Mev. Multiplying by 4π gives a total cross section of 5×10^{-29} cm^2 with about 25% statistical error.

The desired information, for purposes of making the correction, is the proton energy spectrum as a function of angle and machine energy. Since so little is known about the interaction one must begin by making assump-

TABLE I. Experimental results. Columns are: proton laboratory angle in degrees, central photon energy in Mev, differential cross section in c.m. system in units of 10^{-30} cm^2/sterad, Type I error in percent, Type II error in percent, combined Type I and Type II errors, pair process correction factor (multiplying by this factor gives uncorrected cross section), absorption correction factor (dividing by this factor gives uncorrected cross section).

θ_p	k	$d\sigma/d\Omega'$	Type I	Type II	I+II	Pair	Abs.
19	599	2.35	9.4	10.2	13.9	1.38	1.59
21	613	2.28	10.6	10.8	15.1	1.41	1.59
19	702	2.37	8.5	14.2	16.5	1.54	1.98
19	804	3.07	7.9	11.6	14.0	1.41	2.48
30	600	3.52	7.3	4.9	8.8	1.15	1.41
30	709	4.19	5.8	4.2	7.2	1.08	1.81
30	765	3.96	5.6	4.1	6.9	1.00	1.64
30	793	3.72	5.5	4.6	7.2	1.06	1.89
40	601	3.50	5.6	2.8	6.3	1.00	1.24
40	699	4.50	5.6	3.0	6.4	1.01	1.35
40	795	3.90	5.7	3.6	6.8	1.07	1.49
50	600	2.91	5.8	2.7	6.4	1.00	1.12
50	695	3.92	5.9	2.7	6.5	1.00	1.16
50	795	3.66	7.0	2.8	7.5	1.00	1.23
60	600	2.16	7.2	2.6	7.7	1.00	1.05
60	700	2.30	7.0	2.6	7.5	1.00	1.07
60	800	2.11	7.2	2.6	7.7	1.00	1.09

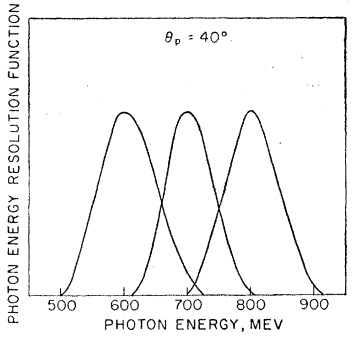

FIG. 5. Photon energy resolution functions for proton laboratory angle of 40°.

[9] Fernbach, Serber, and Taylor, Phys. Rev. **75**, 1352 (1949).

[10] B. Rossi, *High-Energy Particles* (Prentice-Hall, Inc., New York, 1952), p. 347.

[11] M. L. Goldberger, Phys. Rev. **74**, 1269 (1948).

[12] Millburn, Birnbaum, Crandall, and Schecter, Phys. Rev. **95**, 1268 (1954).

[13] M. Bloch and M. Sands, Phys. Rev. **113**, 305 (1959).

tions and determine later their reasonableness. The assumptions used here are: (1) the proton angular distribution is isotropic in the c.m. system, and (2) the matrix element for the photoproduction process is independent of proton energy so that the proton energy spectrum is proportional to the phase-space factor. With these assumptions and the total cross section of Bloch, the proton counting rate due to the process $\gamma+p\rightarrow p+\pi^+\pi^-$ is calculable. Using the phase space factor calculated by Berman, Vette and Walker have developed a code to enable the Datatron digital computer to evaluate the integrals necessary in calculating the counting rate.

The process $\gamma+p\rightarrow p+\pi^0+\pi^0$ also produces recoil protons and must be taken into account. No experimental data exist for this process, so the same assumptions are made as for the π^+, π^- process. Thus, to take the π^0, π^0 process into account, Bloch's total cross section σ_{Tp} is replaced by $\sigma_{Tp}(1+a)$, where a is a constant which must be determined experimentally.

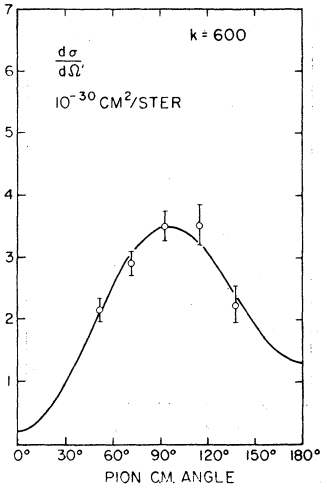

FIG. 6. Angular distribution in center-of-momentum system at laboratory photon energy of 600 Mev. Errors on points are combined Type I and Type II as defined in text. Curves are least-squares fits of the form $A+B\cos\theta+C\cos^2\theta$.

To check the model and determine a value for a, a series of measurements was made to determine the effect of pair production on proton counting rates. This was done by setting the telescope for a given energy and angle and making runs with different values of E_0, the machine energy. Figure 4 shows the results of one of the two sets of runs converted into cross sections with and without the pair correction. The other set of runs shows the same effect. On the basis of these measurements, it was decided that $a=1$ should be used in making corrections to the data. This is in disagreement with Vette,[4] who concluded that $a=0$ should be used.

As far as the recoil proton is concerned, the kinematics of Compton scattering and single pion photoproduction are very similar. Thus, nearly the same photon energy is required to produce a proton of given energy and angle by either process. Measurements of the Compton scattering cross section made up to photon energies of 270 Mev indicate that it is about 1% of the π^0 photo-

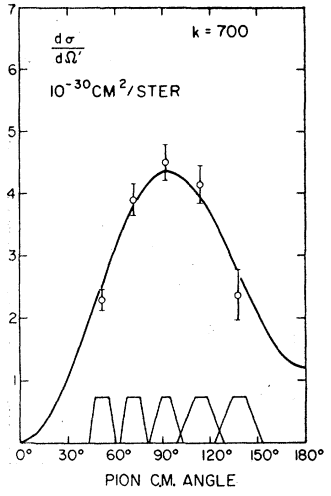

FIG. 7. Angular distribution at 700 Mev. Angular resolution functions are shown at the bottom of the figure.

production cross section at the same energy.[14] A calculation of the Compton cross section by Mathews[15] in the same region based on dispersion theory indicates a relationship between Compton scattering and π^0 photoproduction. For this reason it is considered unlikely that the Compton cross section exceeds a few percent of the π^0 cross section in the region under consideration in this experiment and no correction has been made.

Scattering corrections in this experiment are just small enough to be disregarded. The following effects have been considered and found to produce errors somewhat less than a percent in the most unfavorable case: (1) lateral "wander" of particles in the copper absorber stack, (2) scattering in absorbers A and B, and (3) scattering in the target.

Two sources of error ascribable to electronic equip-

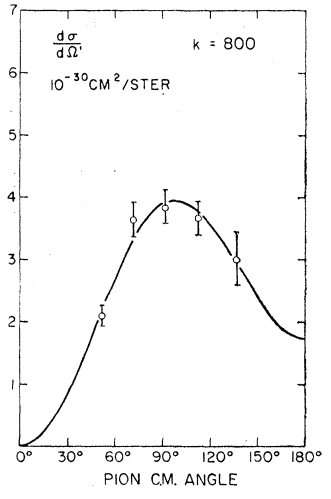

FIG. 8. Angular distribution at 800 Mev.

[14] Auerbach, Bernardini, Filosofo, Hanson, Odian, and Yamagata, *Proceedings of the Cern Symposium on High-Energy Accelerators and Pion Physics, Geneva, 1956* (European Organization of Nuclear Research, Geneva, 1956), Vol. 2, p. 291.

[15] J. Mathews, Ph.D. thesis, California Institute of Technology, 1957 (unpublished).

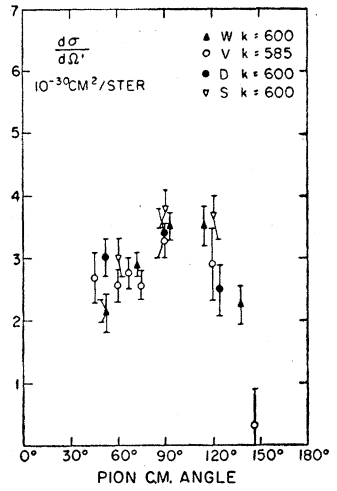

FIG. 9. Angular distribution from this experiment at 600 Mev plotted with angular distribution of Vette, Stein, and Rogers, and DeWire *et al.*

ment have been examined. The first is dead-time loss and the second is accidental coincidences. Both of these produce errors of about a percent in the worst case and are not corrected for.

A "true" counting rate obtained from the data is related to the cross section by the following expression:

$$C=\frac{d\sigma}{d\Omega'}\int dxdydzd\Omega dk\frac{d\Omega'}{d\Omega}\frac{U}{E_0}\frac{B(k,E_0)}{k}n(x,y)N,$$

where C=counting rate in counts/BIP, $d\sigma/d\Omega'$ is the average cross section over the angular and energy ranges defined by the target-telescope system, $d\Omega'/d\Omega$ is the solid angle transformation from the center of momentum system to the laboratory system at constant k, $(U/E_0)B(k,E_0)/k$ gives the photon beam spectrum and normalization as explained earlier, $n(x,y)$ contains the beam intensity variation over the target volume, and $N=4.39\times10^{22}$ is the number of target nuclei per cc. The integral is carried over the target volume, the telescope solid angle, and the photon energy. In certain regions

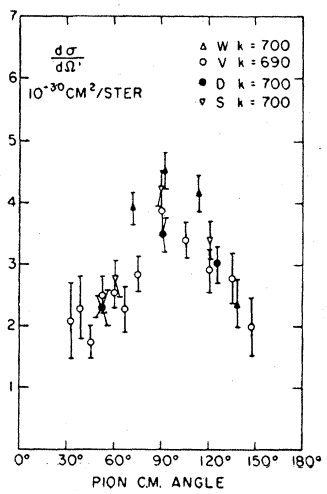

FIG. 10. Angular distribution from this experiment at 700 Mev plotted with angular distribution of Vette, Stein, and Rogers, and DeWire *et al.*

the evaluation of the integral is complicated by the variation over the target volume of proton energy loss in hydrogen, solid angle subtended by telescope, and photon energy for given proton energy. In addition, operating near the bremsstrahlung cutoff causes $B(k,E_0)$ to vary greatly. For reasons of this sort, the integral was evaluated numerically on the Caltech Datatron digital computer by M. Ernstene and the author.

The photon energy resolution function is obtained by performing all the integrations but the one over k. Figure 5 shows some typical resolutions functions. At $\theta_p=20°$ they are roughly half as wide and at $\theta_p=60°$ they are almost twice as wide.

IV. RESULTS AND ERRORS

Sources of error have been classified into three groups according to the way in which they affect the results of the experiment. Below are listed the groups, the

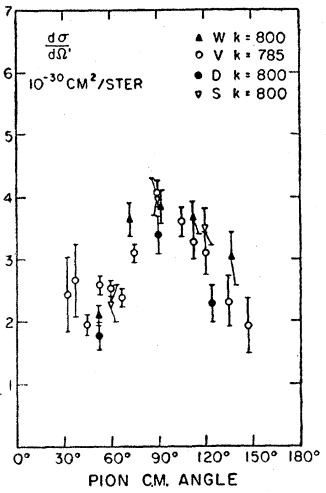

FIG. 11. Angular distribution from this experiment at 800 Mev plotted with angular distribution of Vette, Stein, and Rogers, and DeWire *et al.*

members of each group, and the estimated standard deviation due to each member.

I. Errors which vary randomly from point to point.
   1. Counting statistics: 5% to 7%.
   2. Uncertainty in separating proton peak from meson peak: 2%.
   3. Variations in E_0, P, T, not taken into account by the periodic monitoring: 1%.

II. Errors which vary smoothly from point to point.
   1. Nuclear absorption: 0% to 5%. (5% of the correction).
   2. Pion pairs: 0% to 14% (25% of the correction).
   3. Uncertainty in range, ΔR and $\Delta\Omega$: 1.5% each.
   4. Neglect of Compton scattering: −3% (not included in calculating errors).

III. Errors which are constant for all points.
   1. Beam calibrations: <3%.

Table I presents the cross section values obtained in the experiment with their Type I and Type II errors

and pair and absorption corrections. Table II presents the cross sections used in generating angular distributions. Small interpolations were necessary to obtain cross sections at the desired energies. The measurements at 19° and 21° near $k=600$ Mev have been combined. Figures 6 to 8 exhibit the desired angular distributions. Through a least-squares analysis, coded for the Datatron by J. I. Vette and W. Wales, the data of Table II have been used to determine angular distribution functions of the form $A+B\cos\theta+C\cos^2\theta$. At $k=700$ and 800 Mev, a constraint had to be added to force the angular distribution function to be non-negative at all angles. This was done by introducing a vanishing cross section at zero degrees, thus forcing the function to pass through zero. In the pion momentum range involved it would be reasonable to expect angular momenta of $l>1$ to be present, but the form assuming only $l=0,1$ was used since (1) it gives a satisfactory fit to the data,

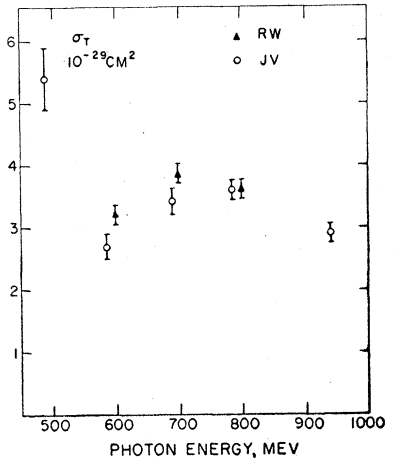

FIG. 12. Total cross-section results of this experiment with those of Vette.

and (2) the data are not sufficiently detailed to provide a good determination of higher order terms.

Table III exhibits the A, B, and C coefficients (in units of 10^{-30} cm^2/sterad) as well as the total cross section $\sigma_T=4\pi(A+C/3)$ (units of 10^{-30} cm^2).

Figures 9 to 11 present the angular distributions of this experiment with those of Vette,[4] Stein and Rogers,[16] and DeWire *et al.*[17] In general, the agreement is fairly satisfactory. No serious discrepancies are found in the

[16] P. C. Stein and K. C. Rogers, Phys. Rev. **110**, 1209 (1958).
[17] DeWire, Jackson, and Littauer, Phys. Rev. **110**, 1208 (1958).

TABLE II. Angular distribution results. Columns are: central photon energy in Mev, meson angle in c.m. system, differential cross section in c.m. system in units of 10^{-30} cm^2/sterad, Type I errors and combined Type I and Type II errors, both in units of 10^{-30} cm^2/sterad.

k	$\theta_{\pi'}$	$d\sigma/d\Omega'$	Type I	I+II
600	138	2.24	±0.16	±0.29
	115	3.52	0.26	0.31
	93	3.50	0.20	0.22
	72	2.91	0.17	0.19
	52	2.16	0.16	0.17
700	138	2.37	0.20	0.39
	114	4.16	0.24	0.30
	92	4.50	0.25	0.28
	72	3.91	0.23	0.25
	52	2.30	0.16	0.17
800	137	3.02	0.24	0.42
	113	3.67	0.20	0.26
	92	3.86	0.22	0.26
	72	3.65	0.26	0.27
	52	2.11	0.15	0.16

TABLE III. Angular distribution coefficients. Columns are: central photon energy in Mev, A, B, and C coefficients in units of 10^{-30} cm^2/sterad, and total cross section in units of 10^{-30} cm^2.

k	A	B	C	σ_T
600	3.47±0.16	−0.55±0.21	−2.70±0.53	32.2±1.4
700	4.31±0.14	−0.60±0.24	−3.70±0.29	38.7±1.5
800	3.88±0.14	−0.87±0.25	−3.00±0.29	36.2±1.5

600-Mev and 800-Mev angular distributions. The worst disagreement appears between the results of this experiment and those of Vette at $k=700$ Mev, pion angles between 60° and 120°. When disagreements first began to appear, both experiments were set up to count protons of the same energy and angle from carbon and were able to agree very well on the number of protons per BIP per Mev per steradian. This would tend to indicate that the discrepancy may arise in the response of one of the experiments to background radiation.

Figure 12 shows the total-cross-section results of this experiment with those of Vette.

ACKNOWLEDGMENTS

The author wishes to thank Professor Alvin V. Tollestrup, Professor Arthur B. Clegg, and Professor Robert L. Walker for their helpful suggestions and assistance during the design, execution, and analysis of this experiment. The continual interest and support of Professor Robert F. Bacher is gratefully acknowledged.